Electronic Supplementary Material (ESI) for New Journal of Chemistry.

Magnetic Investigation in Di- and Tetranuclear Lanthanide Complexes

Jianfeng Wu,[a] ‡ Dan Liu,[b] ‡ Qianqian Yang,[c] Yan Ge,[a] Jinkui Tang[c] and Zhenhui Qi*[a]*

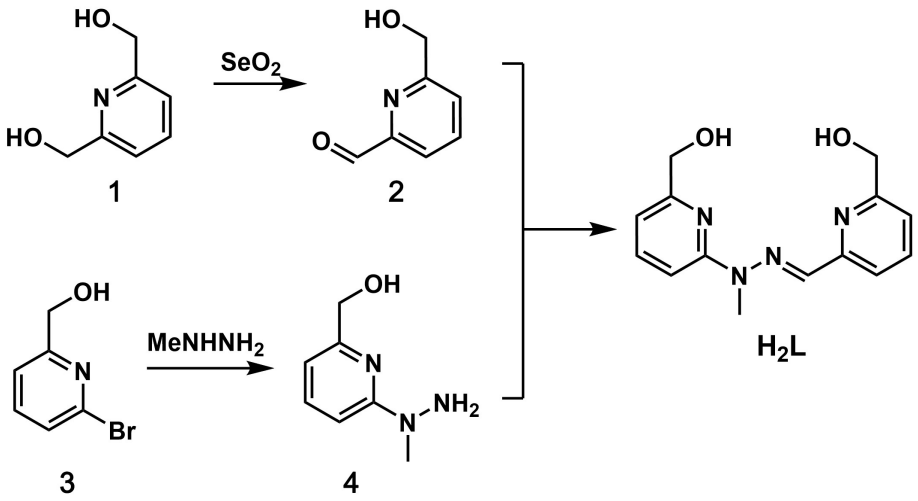

Scheme S1. Schematic drawings of the synthetic route of ligand **H_2L**.

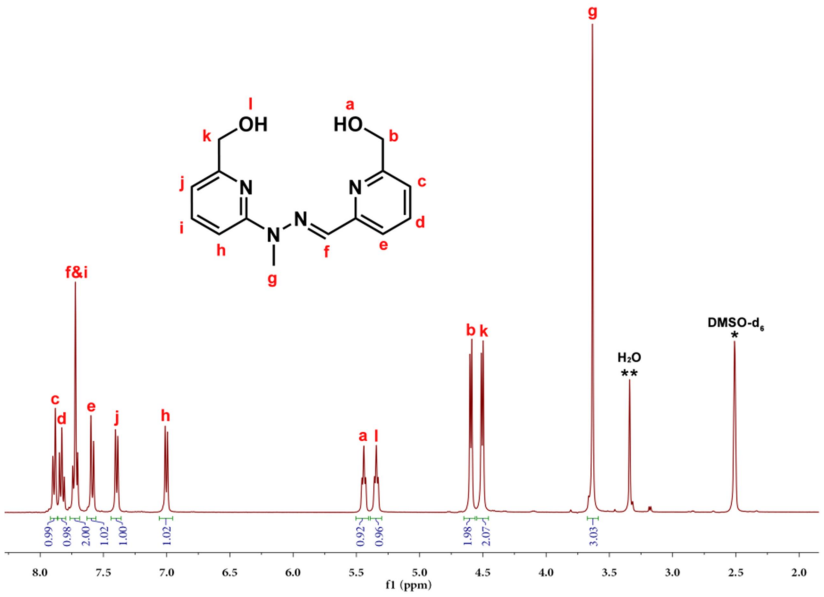

Fig. S1. ^{1}H-NMR spectrum of **H_2L** in DMSO-d_6 recorded at room temperature. Solvent peaks are marked with asterisks (DMSO-d_6, *; H_2O, **).

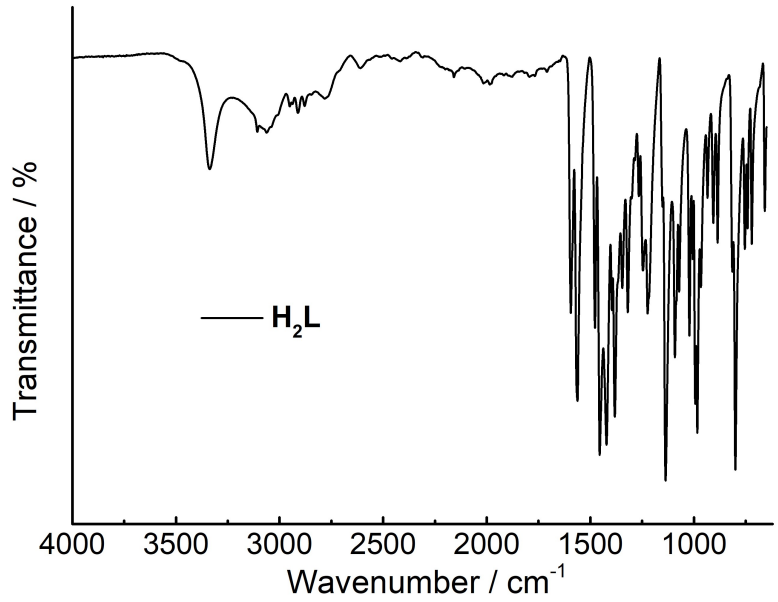

Fig. S2 IR(ATR) spectrum of solid samples for complex **H_2L**.

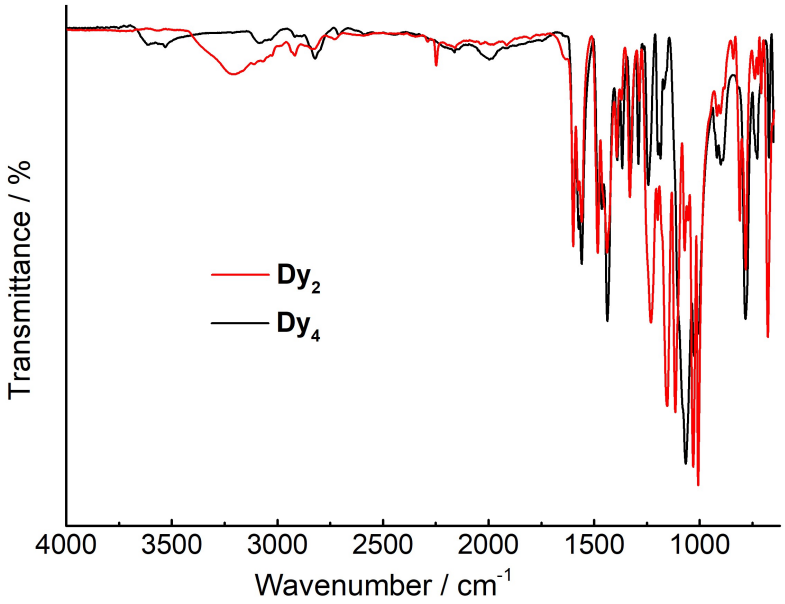

Fig. S3. IR(ATR) spectrum of solid samples for complexes **Dy_2** and **Dy_4**.

Table S1. Crystallographic data of complexes **Dy_2** and **Dy_4**.

	Dy_2	**Dy_4**
empirical formula	$C_{62}H_{69}Dy_2N_{11}O_{17}S_4$	$C_{56}H_{57}Cl_3Dy_4N_{16}O_{21}$
formula weight, g·mol^{-1}	1693.52	2046.52
crystal size, mm³	0.16 × 0.15 × 0.15	0.2 × 0.19 × 0.18
crystal system	Triclinic	Tetragonal
space group	*P*-1	*P4/mcc*
T, K	180.0	173.0
λ, Å	1.54178	1.54178
a, Å	13.8109(8)	11.6051(5)
b, Å	14.5458(8)	11.6051(5)
c, Å	18.5543(10)	25.651(3)
α, °	85.497(3)	90
β, °	79.190(3)	90
γ, °	75.155(3)	90
V, Å^3	3537.2(3)	3454.6(5)
Z	2	2
ρ (cal), g·cm^{-3}	1.590	1.967
F(000)	1700.0	1976.0
2θ range [°]	4.85 to 124.868	10.78 to 125.316
*T*max / *T*min	0.191 / 0.145	0.018 / 0.012
measured refl.	33743	8562
unique refl. [*R*int]	10945, 0.0815	1409, 0.0992
goodness-of-fit (F^2)	1.055	1.119
data / restr. / param.	10945 / 1319 / 918	1409 / 271 / 130
*R*1, *wR*2 ($I > 2\sigma(I)$)	0.0976, 0.2168	0.1185, 0.2509
*R*1, *wR*2 (all data)	0.1183, 0.2307	0.1587, 0.2773
res. el. dens. [e·Å^{-3}]	2.11 / -1.64	1.39 / -1.10

Table S2. Selected bond distances (Å) and angles (°) in complex **Dy_2**.

Dy1-O1	2.438(7)	Dy2-O3	2.275(8)	O1-Dy1-N4	70.2(3)	O3-Dy2-O5	69.0(3)
Dy1-O2	2.436(8)	Dy2-O4	2.230(9)	O2-Dy1-N1	62.9(3)	O3-Dy2-O6	79.4(3)
Dy1-O3	2.266(8)	Dy2-O5	2.443(10)	O3-Dy1-O1	81.3(3)	O4-Dy2-O3	68.3(3)
Dy1-O4	2.349(8)	Dy2-O6	2.356(10)	O3-Dy1-O2	96.5(3)	O4-Dy2-O9	86.7(3)
Dy1-O12	2.403(9)	Dy2-O9	2.352(9)	O3-Dy1-O4	66.5(3)	O4-Dy2-N5	66.8(3)
Dy1-O15	2.405(8)	Dy2-N5	2.488(9)	O3-Dy1-O15	80.7(3)	O5-Dy2-N8	63.8(3)
Dy1-N1	2.568(9)	Dy2-N8	2.525(9)	O3-Dy1-N4	66.3(3)	O6-Dy2-N5	90.7(4)
Dy1-N4	2.506(10)	Dy2-N3A	2.590(17)	O4-Dy1-O1	75.7(3)	O6-Dy2-N8	82.2(4)
Dy1-N0A	2.559(15)			O4-Dy1-O2	67.9(3)	O9-Dy2-O5	76.8(3)
				O4-Dy1-O12	83.2(3)	O9-Dy2-N5	76.4(3)
				O12-Dy1-O1	68.8(3)	O9-Dy2-N8	80.3(4)
				O12-Dy1-O2	92.6(3)	O9-Dy2-N3A	82.4(15)
				O12-Dy1-N1	65.6(3)	N5-Dy2-N3A	61.9(6)
				O15-Dy1-O2	75.9(3)	N8-Dy2-N3A	61.1(7)
				O15-Dy1-N1	72.7(3)		
Dy1-Dy2	3.7848(10)			O15-Dy1-N4	70.6(3)		

Table S3. Selected bond distances (Å) and angles (°) in complex **Dy_4**.

Dy1-O2$^{\#1}$	2.339(16)	Dy1-O1-Dy$^{\#1}$	90
Dy1-O2	2.282(15)	O2-Dy1-O2$^{\#1}$	69.4(8)
Dy1-O1	2.4646(16)	O2$^{\#4}$-Dy1-O2	71.4(8)
Dy1-N3	2.57(2)	O2$^{\#2}$-Dy1-O1	71.5(4)
Dy1-N1	2.463(12)	O2-Dy1-O1	72.4(4)
		O2$^{\#2}$-Dy1-N3	93.5(6)
		O2-Dy1-N1	66.9(5)
		O2$^{\#2}$-Dy1-N1	77.7(5)
Dy1-Dy1$^{\#1}$	3.485(2)	N1-Dy1-N3	60.4(4)

$^{\#1}$ +Y, 1-X, 1-Z, $^{\#2}$ 1-Y,+X,+Z, 1-Z, $^{\#3}$ 1-Y,+X,1-Z, $^{\#4}$ +X,+Y,1-Z

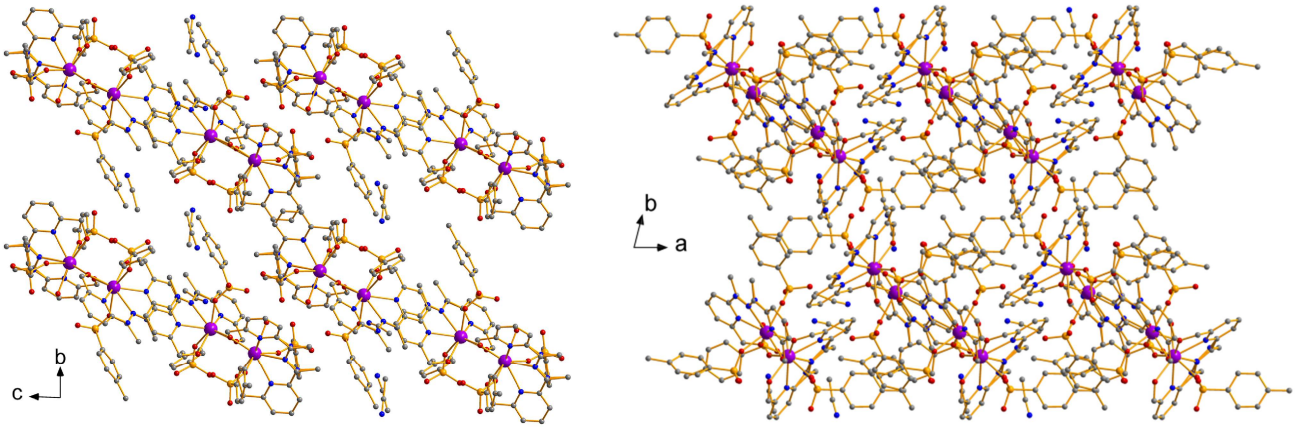

Fig. S4 Packing model along with *a* and *c* axes of complex **Dy_2**. The purple, orange, gray, blue, and red spheres representing Dy, S, C, N, and O, respectively; hydrogen atoms have been omitted for clarity.

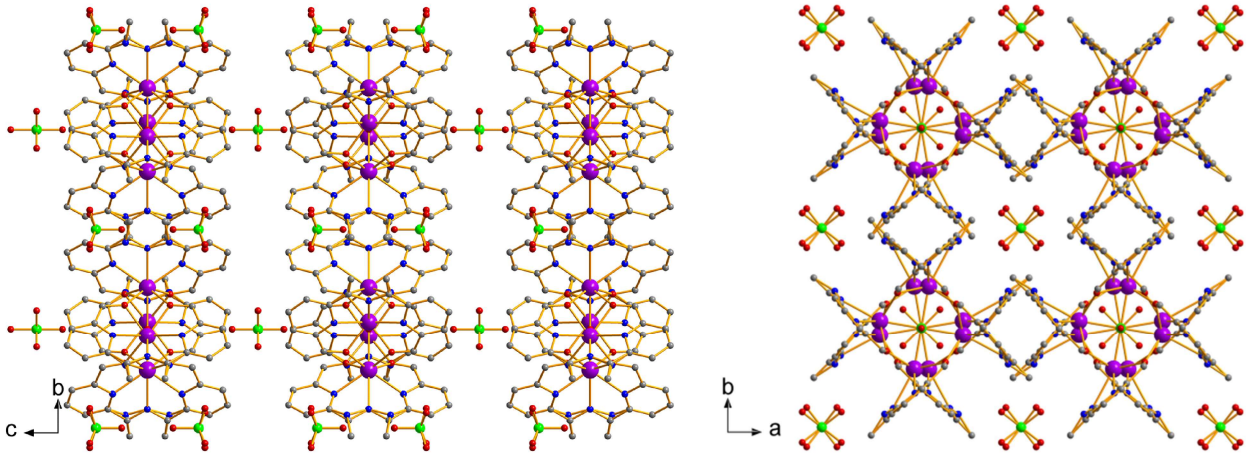

Fig. S5 Packing model along with *a* and *c* axes of complex **Dy_4**. The purple, green, gray, blue, and red spheres representing Dy, Cl, C, N, and O, respectively; hydrogen atoms have been omitted for clarity.

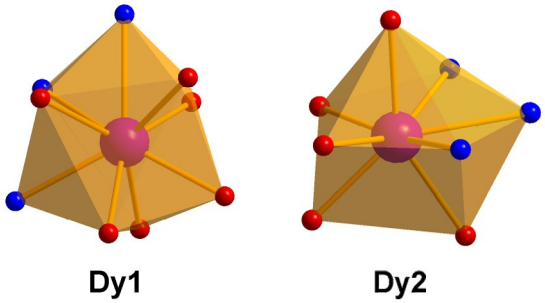

Fig. S6 Coordination polyhedrons of Dy1 (left) and Dy2 (right) in complex **Dy_2**.

Table S4. The *CShM* values calculated by *SHAPE* 2.1 of Dy^{III} ions in **Dy_2**.

Coordination Geometry	Dy1	Coordination Geometry	Dy2
Johnson triangular cupola (C_{3v})	14.670	Cube (O_h)	13.091
Capped cube (C_{4v})	11.440	Square antiprism (D_{4d})	9.890
Spherical-relaxed capped cube (C_{4v})	10.653	Triangular dodecahedron (D_{2d})	8.814
Capped square antiprism (C_{4v})	6.432	Johnson gyrobifastigium J26 (D_{2d})	5.080
Spherical capped square antiprism (C_{4v})	5.407	Elongated triangular bipyramid (D_{3h})	22.200
Tricapped trigonal prism (D_{3h})	4.829	Biaugmented trigonal prism (C_{2v})	5.889
Spherical tricapped trigonal prism (D_{3h})	6.217	Snub diphenoid J84 (D_{2d})	5.591

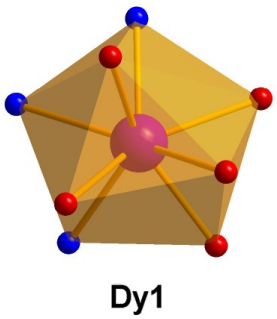

Fig. S7 Coordination polyhedron of Dy1 in complex **Dy_4**.

Table S5. The *CShM* values calculated by *SHAPE* 2.1 of Dy^{III} ion in **Dy_4**.

Coordination Geometry	Dy1
Cube (O_h)	25.827
Square antiprism (D_{4d})	15.529
Triangular dodecahedron (D_{2d})	16.735
Johnson gyrobifastigium J26 (D_{2d})	17.357
Elongated triangular bipyramid (D_{3h})	18.971
Biaugmented trigonal prism (C_{2v})	13.925
Snub diphenoid J84 (D_{2d})	15.520

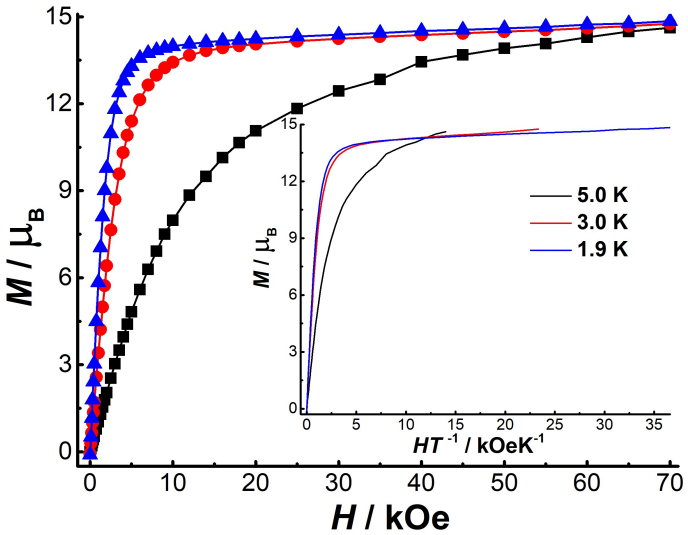

Fig. S8 Molar magnetization (*M*) *vs*. magnetic field (*H*) for **Dy2** at 1.9, 3.0, and 5.0 K.

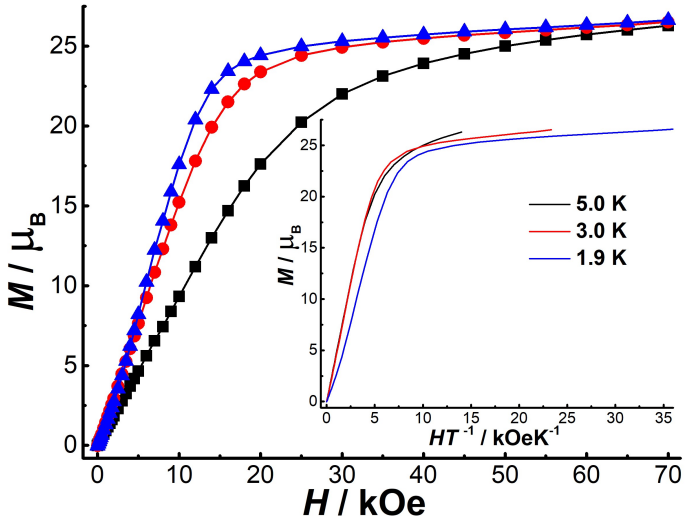

Fig. S9 Molar magnetization (*M*) *vs*. magnetic field (*H*) for **Dy4** at 1.9, 3.0, and 5.0 K.

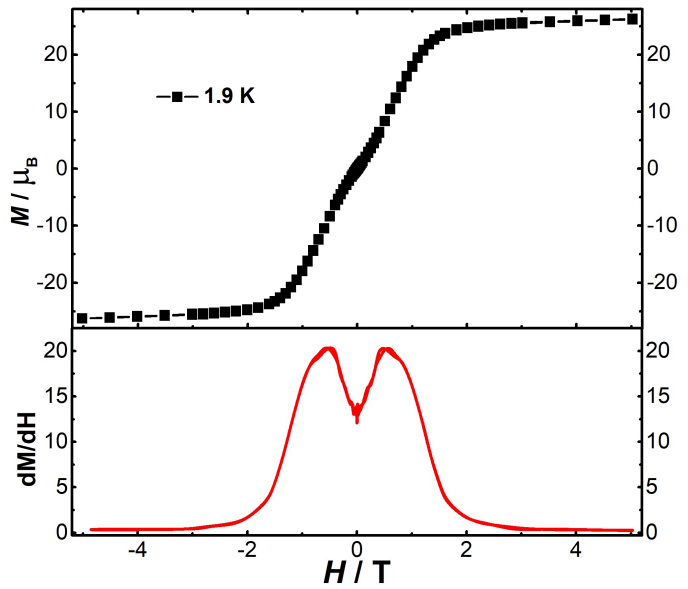

Fig. S10 Molar magnetization (*M*) *vs*. field (*H*) and the relevant differentiate plot of d*M*/d*H* *vs*. *H* for **Dy4** at 1.9 K in range of -5 to 5 T.

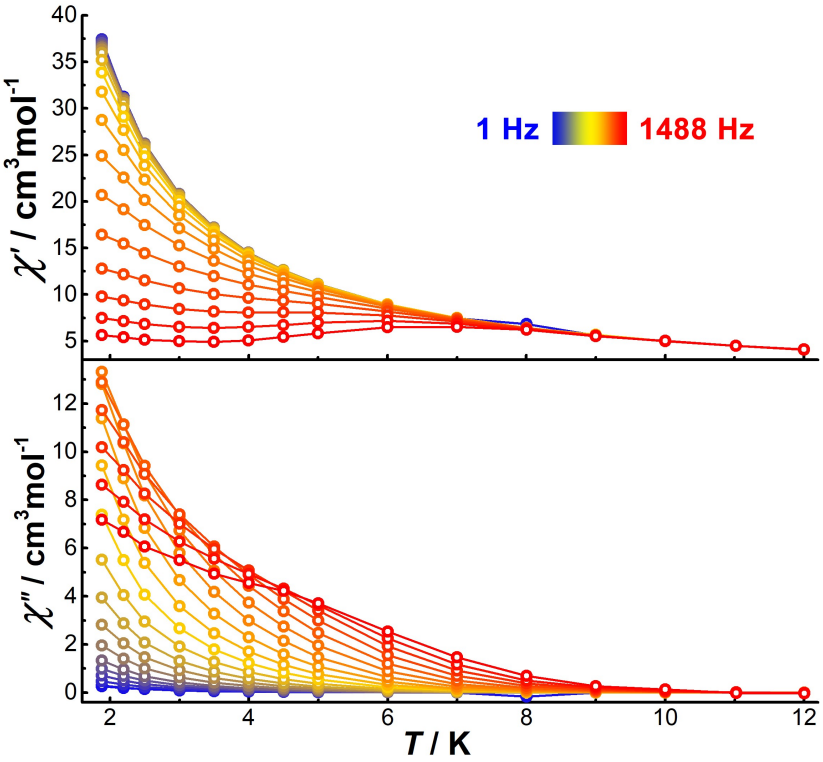

Fig. S11 Temperature-dependent ac susceptibility of **Dy_2** under zero dc field.

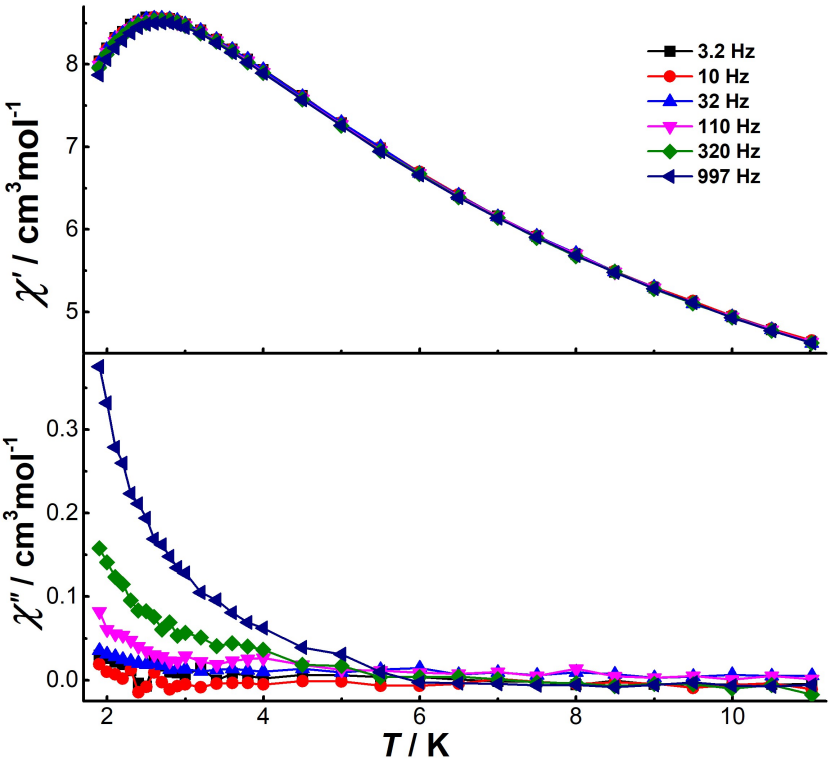

Fig. S12 Temperature-dependent ac susceptibility of **Dy_4** under 1500 Oe dc field.

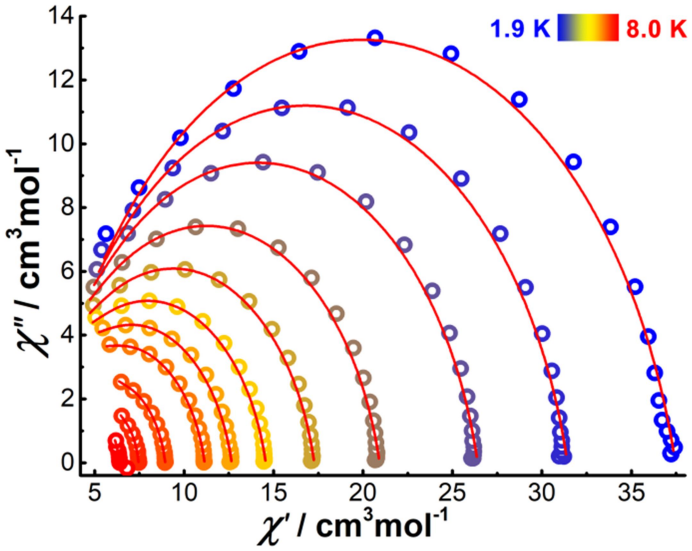

Fig. S13 Cole-Cole plots for **Dy_2** under zero dc field at indicated temperatures. The red lines represent the best fitting.

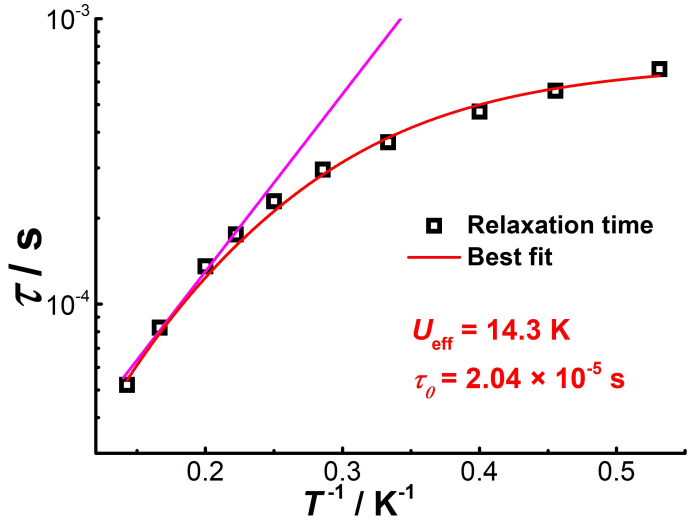

Fig. S14 Plot of τ *vs.* T^{-1} for **Dy_2** obtained under zero dc fields. The red and pink lines represent the fit.

Table S6. The best fit of frequency-dependent ac susceptibility of **Dy_2** under zero dc field.

T / K	χ_S	χ_T	τ / s	α	*Residual*
1.88173	2.38296	37.4804	6.64245E-4	0.16884	0.271649
2.19573	2.18388	31.4499	5.57964E-4	0.16095	0.213507
2.49918	1.95592	26.4298	4.71733E-4	0.15848	0.1293
3.00034	1.61742	20.9524	3.68456E-4	0.15943	0.079513
3.49951	1.56937	17.2989	2.95425E-4	0.15472	0.039799
3.99736	1.43816	14.5909	2.28787E-4	0.15706	0.24979
4.50052	1.4906	12.6883	1.75188E-4	0.15678	0.18481
4.99991	1.77171	11.1736	1.35511E-4	0.15087	0.09262
5.9997	2.63972	8.9706	8.25862E-5	0.12803	0.02804
7	3.44658	7.47739	5.20434E-5	0.0892	0.00469

Table S7. Contractions of the employed three basis sets in different computational approximations for these two compounds.

Basis 1	Basis 2	Basis 3
Dy.ANO-RCC-VDZP	Dy.ANO-RCC-VDZP	Dy.ANO-RCC-VTZP
Lu.ANO-RCC-VDZ	Lu.ANO-RCC-VDZP	Lu.ANO-RCC-VDZP
S.ANO-RCC-VDZ	S.ANO-RCC-VDZP	S.ANO-RCC-VDZP
O.ANO-RCC-VDZ	O.ANO-RCC-VDZP	O.ANO-RCC-VDZP
N.ANO-RCC-VDZ	N.ANO-RCC-VDZP	N.ANO-RCC-VDZP
C.ANO-RCC-VDZ	C.ANO-RCC-VDZ	C.ANO-RCC-VDZ
H.ANO-RCC-VDZ	H.ANO-RCC-VDZ	H.ANO-RCC-VDZ

Table S8. Spin-orbit energies of the lowest Kramer doublets (KDs) (cm^{-1}) calculated with different basis sets for Dy^{III} ions in **Dy_2**.

Basis 1		Basis 2		Basis 3	
Dy1	Dy2	Dy1	Dy2	Dy1	Dy2
0.000	0.000	0.000	0.000	0.000	0.000
81.420	92.662	88.484	82.934	91.467	84.050
131.348	158.003	139.083	129.060	142.481	133.674
169.563	238.971	177.436	218.469	180.624	223.372
248.807	333.307	251.488	303.077	255.292	310.571
312.608	416.567	306.368	380.965	310.661	390.157
350.280	480.637	346.341	449.914	353.363	462.573
503.944	547.918	494.567	519.279	503.725	535.716

Table S9. The *g* tensors of the lowest Kramer doublets (KDs) calculated with different basis sets for Dy^{III} ions in **Dy_2**.

KD		Basis 1		Basis 2		Basis 3	
		Dy1	Dy2	Dy1	Dy2	Dy1	Dy2
1	g_X	0.018	0.039	0.033	0.057	0.031	0.057
	g_Y	0.042	0.065	0.068	0.103	0.063	0.103
	g_Z	18.882	19.366	18.813	19.239	18.823	19.216
2	g_X	0.314	0.473	0.423	0.733	0.421	0.668
	g_Y	0.638	0.635	0.812	1.253	0.808	1.100
	g_Z	17.701	17.608	17.028	16.770	17.008	16.809
3	g_X	1.776	0.621	1.569	0.079	1.594	0.056
	g_Y	4.838	1.613	4.812	1.812	4.970	1.738
	g_Z	14.180	15.123	14.081	14.740	13.946	14.746
4	g_X	2.167	1.051	1.677	1.223	1.733	1.261
	g_Y	4.785	3.356	4.978	3.177	5.067	3.194
	g_Z	9.918	11.212	10.274	11.836	10.169	11.761

Table S10. The KD wavefunctions of the Dy^{III} centers calculated with basis 3 for complex **Dy_2**.

KD	Dy1	Dy2
1	$79.6\%\left\vert\pm\frac{15}{2}\right\rangle+14.4\%\left\vert\pm\frac{11}{2}\right\rangle$	$88.9\%\left\vert\pm\frac{15}{2}\right\rangle$
2	$55.5\%\left\vert\pm\frac{13}{2}\right\rangle+13.1\%\left\vert\pm\frac{11}{2}\right\rangle+15.2\%\left\vert\pm\frac{9}{2}\right\rangle$	$17.1\%\left\vert\pm\frac{13}{2}\right\rangle+34.4\%\left\vert\pm\frac{9}{2}\right\rangle+25.9\%\left\vert\pm\frac{7}{2}\right\rangle+12.4\%\left\vert\pm\frac{5}{2}\right\rangle$
3	$13.4\%\left\vert\pm\frac{11}{2}\right\rangle+27.3\%\left\vert\pm\frac{9}{2}\right\rangle+12.5\%\left\vert\pm\frac{7}{2}\right\rangle+15.8\%\left\vert\pm\frac{5}{2}\right\rangle+12.3\%\left\vert\pm\frac{3}{2}\right\rangle$	$31.4\%\left\vert\pm\frac{13}{2}\right\rangle+22.7\%\left\vert\pm\frac{11}{2}\right\rangle+12.2\%\left\vert\pm\frac{9}{2}\right\rangle+19.5\%\left\vert\pm\frac{7}{2}\right\rangle$
4	$17.6\%\left\vert\pm\frac{13}{2}\right\rangle+18.3\%\left\vert\pm\frac{11}{2}\right\rangle+16.5\%\left\vert\pm\frac{9}{2}\right\rangle+20.8\%\left\vert\pm\frac{7}{2}\right\rangle$	$16.2\%\left\vert\pm\frac{13}{2}\right\rangle+25.7\%\left\vert\pm\frac{11}{2}\right\rangle+25.2\%\left\vert\pm\frac{5}{2}\right\rangle+19.6\%\left\vert\pm\frac{3}{2}\right\rangle$
5	$12.2\%\left\vert\pm\frac{11}{2}\right\rangle+36.8\%\left\vert\pm\frac{7}{2}\right\rangle+13.5\%\left\vert\pm\frac{5}{2}\right\rangle+17.2\%\left\vert\pm\frac{3}{2}\right\rangle$	$24.3\%\left\vert\pm\frac{13}{2}\right\rangle+20.1\%\left\vert\pm\frac{9}{2}\right\rangle+12.1\%\left\vert\pm\frac{7}{2}\right\rangle+19.3\%\left\vert\pm\frac{3}{2}\right\rangle+16.2\%\left\vert\pm\frac{1}{2}\right\rangle$
6	$28\%\left\vert\pm\frac{5}{2}\right\rangle+43.2\%\left\vert\pm\frac{1}{2}\right\rangle$	$14.6\%\left\vert\pm\frac{11}{2}\right\rangle+16.6\%\left\vert\pm\frac{7}{2}\right\rangle+16.5\%\left\vert\pm\frac{5}{2}\right\rangle+10.1\%\left\vert\pm\frac{3}{2}\right\rangle+39.4\%\left\vert\pm\frac{1}{2}\right\rangle$
7	$18.2\%\left\vert\pm\frac{5}{2}\right\rangle+43.5\%\left\vert\pm\frac{3}{2}\right\rangle+21.6\%\left\vert\pm\frac{1}{2}\right\rangle$	$14.3\%\left\vert\pm\frac{9}{2}\right\rangle+19.2\%\left\vert\pm\frac{5}{2}\right\rangle+25.2\%\left\vert\pm\frac{3}{2}\right\rangle+15.9\%\left\vert\pm\frac{1}{2}\right\rangle$
8	$15.3\%\left\vert\pm\frac{11}{2}\right\rangle+23.4\%\left\vert\pm\frac{9}{2}\right\rangle+19.2\%\left\vert\pm\frac{7}{2}\right\rangle+13.5\%\left\vert\pm\frac{5}{2}\right\rangle+11.8\%\left\vert\pm\frac{3}{2}\right\rangle+12.4\%\left\vert\pm\frac{1}{2}\right\rangle$	$12.1\%\left\vert\pm\frac{9}{2}\right\rangle+14.2\%\left\vert\pm\frac{7}{2}\right\rangle+15.8\%\left\vert\pm\frac{5}{2}\right\rangle+21.4\%\left\vert\pm\frac{3}{2}\right\rangle+23.5\%\left\vert\pm\frac{1}{2}\right\rangle$

Table S11. Energies of the lowest Kramer doublets (KDs) (cm^{-1}) calculated with different basis sets for Dy^{III} ion in **Dy_4**.

Spin-orbit energies, cm^{-1}		
Dy1_Basis 1	Dy1_Basis 2	Dy1_Basis 3
0.000	0.000	0.000
39.932	29.701	27.228
78.329	79.810	77.078
132.001	128.532	128.675
205.697	202.393	202.513
272.126	284.714	288.193
325.128	301.583	305.119
346.139	369.010	371.402

Table S12. The *g* tensors of the lowest Kramer doublets (KDs) of Dy^{III} ion in complex **Dy_4**.

KD		Dy1_Basis 1	Dy1_Basis 2	Dy1_Basis 3
		g	***g***	***g***
1	g_X	0.124	2.496	2.790
	g_Y	1.264	2.847	3.207
	g_Z	16.964	15.173	14.617
2	g_X	5.620	8.145	8.478
	g_Y	6.462	6.560	6.266
	g_Z	9.041	3.824	3.400
3	g_X	0.018	0.541	0.721
	g_Y	2.329	1.377	1.497
	g_Z	12.359	11.206	10.901
4	g_X	3.877	4.036	7.996
	g_Y	5.813	5.820	6.467
	g_Z	8.874	8.788	4.090

Table S13. The KD wavefunctions of the Dy center calculated with basis 3 for complex **Dy_4**.

KD	Crystal filed wavefunction
1	$59.1\%\left\|\pm\frac{15}{2}\right\rangle+19.5\%\left\|\pm\frac{9}{2}\right\rangle+10.2\%\left\|\pm\frac{5}{2}\right\rangle$
2	$16.9\%\left\|\pm\frac{13}{2}\right\rangle+29.4\%\left\|\pm\frac{7}{2}\right\rangle+12.4\%\left\|\pm\frac{5}{2}\right\rangle+11.2\%\left\|\pm\frac{3}{2}\right\rangle+13.2\%\left\|\pm\frac{1}{2}\right\rangle$
3	$12.5\%\left\|\pm\frac{15}{2}\right\rangle+11.6\%\left\|\pm\frac{13}{2}\right\rangle+17.1\%\left\|\pm\frac{11}{2}\right\rangle+12\%\left\|\pm\frac{7}{2}\right\rangle+17.5\%\left\|\pm\frac{5}{2}\right\rangle+17.5\left\|\pm\frac{3}{2}\right\rangle$
4	$11.4\%\left\|\pm\frac{15}{2}\right\rangle+14.8\%\left\|\pm\frac{13}{2}\right\rangle+14.7\%\left\|\pm\frac{11}{2}\right\rangle+14\%\left\|\pm\frac{9}{2}\right\rangle+23.9\%\left\|\pm\frac{1}{2}\right\rangle$
5	$25.8\%\left\|\pm\frac{13}{2}\right\rangle+13.1\%\left\|\pm\frac{11}{2}\right\rangle+23.7\%\left\|\pm\frac{3}{2}\right\rangle+20\%\left\|\pm\frac{1}{2}\right\rangle$
6	$11.8\%\left\|\pm\frac{13}{2}\right\rangle+10.5\%\left\|\pm\frac{11}{2}\right\rangle+10.9\%\left\|\pm\frac{9}{2}\right\rangle+18.7\%\left\|\pm\frac{7}{2}\right\rangle+22.3\%\left\|\pm\frac{5}{2}\right\rangle+19.9\%\left\|\pm\frac{1}{2}\right\rangle$
7	$16.3\%\left\|\pm\frac{11}{2}\right\rangle+24.7\%\left\|\pm\frac{9}{2}\right\rangle+24.8\%\left\|\pm\frac{3}{2}\right\rangle+12.8\%\left\|\pm\frac{1}{2}\right\rangle$
8	$16.6\%\left\|\pm\frac{13}{2}\right\rangle+20.9\%\left\|\pm\frac{11}{2}\right\rangle+19\%\left\|\pm\frac{9}{2}\right\rangle+22.3\%\left\|\pm\frac{7}{2}\right\rangle+13.2\%\left\|\pm\frac{5}{2}\right\rangle$

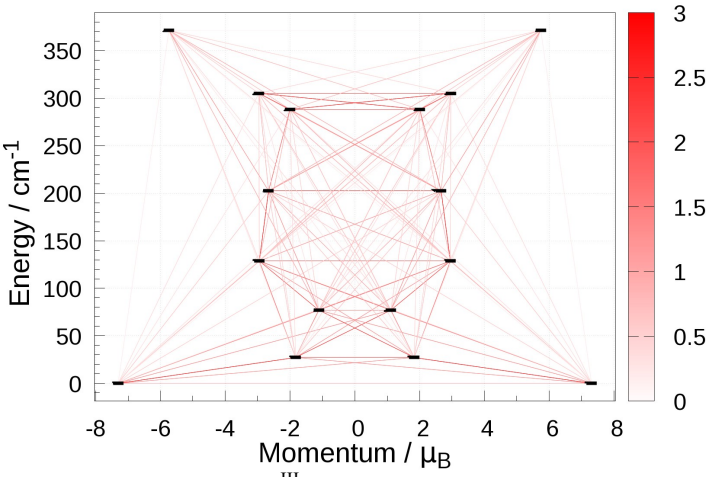

Fig. S15 Magnetization blocking barrier for the Dy^{III} center calculated with basis 3 for **Dy_4**. Each doublet state $\pm M_J$ arising from a given atomic multiplet. $^{2S+1}L_J$ is placed according to its saturation magnetic moment (horizontal axis). The intensity of the pink lines indicates the amplitude of the average transition magnetic dipole moment in μ_B between the connected states (see the legend in the right hand side), the square of which roughly scales with the rat e of spin-phonon transition between them. The most intense lines outline the magnetization blocking barrier (solid red lines).

Table S14. The following matrix based on the ground KDs was used in calculating the dipolar interaction between the Dy^{III} ions in complex **Dy_2**.

$$J = \begin{bmatrix} -0.5678486672200 & 0.01029808818067 & -1.221881250969 \\ 0.2301961139614 & -0.0041399759959 & 0.4952185645259 \\ -2.137392434127 & 0.03870023678896 & -4.599198273416 \end{bmatrix}$$

Table S15. The following matrixes based on the ground KDs were used in calculating the dipolar interaction between the Dy^{III} ions in complex **Dy_4**.

$$J_1 = \begin{bmatrix} -0.3410693622941 & 0.4998510755892 & 0.8660984509601 \\ 0.6230664880840 & -0.51421659781 & -1.212749552340 \\ 0.7805792687558 & -0.81713718173 & -1.410204650935 \end{bmatrix}$$

$$J_2 = \begin{bmatrix} -0.17046349737 & 0.2321639828601 & 0.3444784925054 \\ 0.2321639828601 & -0.398410489422 & -0.6212262095252 \\ 0.3444784925054 & -0.6212262095252 & -0.8618499459774 \end{bmatrix}$$

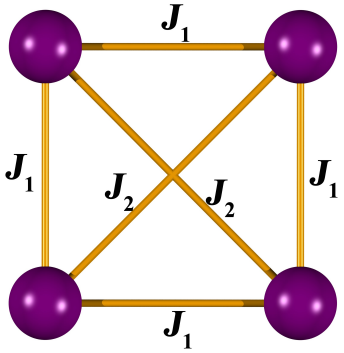

Fig. S16 Magnetic interaction models in complex **Dy_4**.

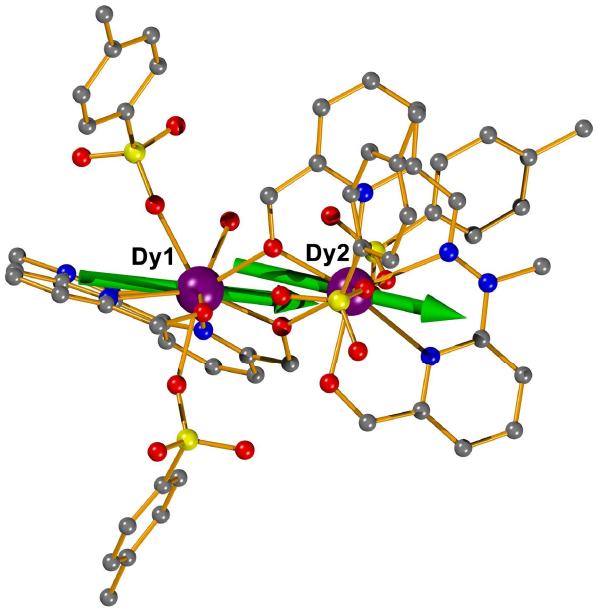

Fig. S17 Calculated orientations of the local main magnetic axes on Dy^{III} ions calculated with basis 3 for **Dy_2** in the ground KDs. The hydrogen atoms have been omitted for clarity.

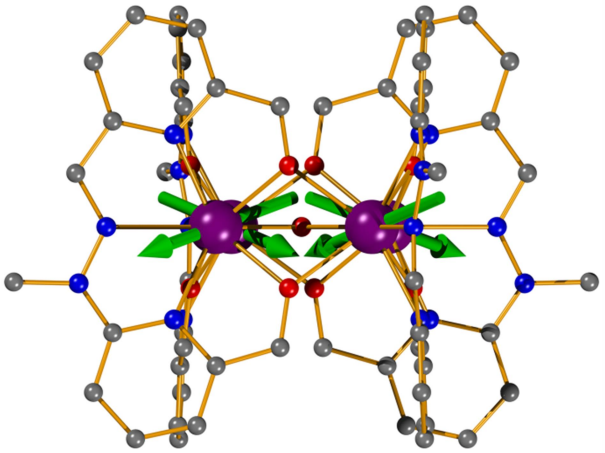

Fig. S18 Calculated orientations of the local main magnetic axes on Dy^{III} ions calculated with basis 3 for **Dy_4** in the ground KDs. The hydrogen atoms have been omitted for clarity.